

1

2 **Supplementary Information for**  
3 **Individual variations lead to universal and cross-species patterns of social behavior**  
4 **Sang Hyun Choi, Vikyath D. Rao, Tim Gernat, Adam Hamilton, Gene E. Robinson, Nigel Goldenfeld**  
5 **Corresponding Author: Nigel Goldenfeld**  
6 **E-mail: [nigel@uiuc.edu](mailto:nigel@uiuc.edu)**

7 **This PDF file includes:**  
8     Supplementary text  
9     Figs. S1 to S5  
10    References for SI reference citations

## Supporting Information Text

### 1. Quantile-quantile plots of the pair interaction time distribution

Our model predicts the pair interaction time distribution to be exponential. We have generated the quantile-quantile (QQ) plots of pair interaction times of honeybees and humans to verify the prediction. If the data followed the proposed probability density, a QQ plot would show a linear line. QQ plot was meant to be a preliminary test to examine the probability density of the pair interaction times, so only a few pairs from each dataset have been tested. The pair with the most number of interactions from each dataset has been chosen to be demonstrated here for clearer examination of the distribution.

As shown in Fig. S1, although some pair interaction times appear to be exponential, there are data that deviate for long times. The deviation is always upward, which implies that it is not due to statistical fluctuations but is instead a systematic effect. The upward deviation indicates that the actual probability density decays more slowly than the proposed one. However, even the deviating data align well with the reference line for short times. The deviating region at long times also looks linear although it does not lie on the reference line. The linearity suggests that the deviating region is exponential as well, but with a slower decaying rate than the short time region. A weighted sum of two exponential distributions, sometimes known as a hyperexponential distribution, exhibits the same behavior. Its limiting behavior at small values of the argument is the faster decaying of the two summed exponentials whilst its limiting behavior at large values is the other one. Therefore, we deduce that the pair interaction time distribution is hyperexponential, and is well approximated by just two terms.

### 2. Calculation of the interaction time distribution.

As discussed in the main text, the probability density of the rates is  $p(\omega) \sim \omega^\alpha$ . Integrating the pair interaction time distribution over the rates gives

$$f(t) = \int_0^\epsilon d\omega p(\omega) f(\omega, t) = \int_0^\epsilon d\omega \omega^{\alpha+1} e^{-\omega t} = t^{-(2+\alpha)} \gamma(2 + \alpha, \epsilon t) \quad [S1]$$

where  $\gamma(a, z) \equiv \int_0^z t^{a-1} e^{-t} dt$  is the incomplete gamma function. Since  $p(\omega) \sim \omega^\alpha$  is for small  $\omega$  limit, the integration is performed up to a finite value  $\epsilon$ .  $\gamma(a, z)$  approaches a constant  $\Gamma(a) \equiv \int_0^\infty t^{a-1} e^{-t} dt$  as  $z \rightarrow \infty$  ( $a$  is fixed in our case), which means that equation S1 would become  $f(t) \sim t^{-(2+\alpha)}$  for large  $\epsilon t$ .  $\gamma(a, z)$  starts to saturate to a constant value at  $z$  of order 1. Therefore, the large  $\epsilon t$  condition translates into  $t > 1/\epsilon$ . We assume  $\epsilon$  to be small, but it is the largest value of  $\omega$  in the population (equation S1). So the condition  $t > 1/\epsilon$  is satisfied for most  $t$ , and we observe the heavy-tailed distribution  $f(t) \sim t^{-(2+\alpha)}$ .

The pair interaction time distribution turns out to be better represented by a hyperexponential distribution than an exponential distribution. However, this modification does not affect the final result  $f(t) \sim t^{-(2+\alpha)}$ . Now the pair interaction time distribution is  $f_{pair}(t) = g\omega_1 e^{-\omega_1 t} + (1-g)\omega_2 e^{-\omega_2 t}$  where  $g$  is a weight on one of the two exponential terms. Since we now have two rates  $\omega_1$  and  $\omega_2$  with relation  $\omega_1 > \omega_2$ , the integration becomes

$$f(t) = \int_0^\epsilon d\omega_1 p(\omega_1) \int_0^{\omega_1} d\omega_2 p(\omega_2) \left\{ g\omega_1 e^{-\omega_1 t} + (1-g)\omega_2 e^{-\omega_2 t} \right\}. \quad [S2]$$

The first term is calculated as

$$\int_0^\epsilon d\omega_1 \omega_1^\alpha \frac{g}{\alpha+1} \omega_1^{\alpha+2} e^{-\omega_1 t} = \frac{g}{\alpha+1} t^{-(3+2\alpha)} \gamma(3+2\alpha, \epsilon t) \sim t^{-(3+2\alpha)}. \quad [S3]$$

The last asymptotic relation is for large  $t$ . Here “large  $t$ ” means  $t > 1/\epsilon$  as stated in the previous paragraph. The first integral of the second term gives us  $(1-g)t^{-(2+\alpha)} \gamma(2+\alpha, \omega_1 t)$ . Then the second term is calculated as

$$(1-g)t^{-(2+\alpha)} \int_0^\epsilon d\omega_1 \omega_1^\alpha \gamma(2+\alpha, \omega_1 t) \sim t^{-(2+\alpha)} \quad [S4]$$

for large  $t$  because  $\gamma(2+\alpha, \omega_1 t)$  is essentially a constant for that limit. Therefore, the interaction time distribution for the whole population becomes

$$f(t) \sim At^{-(3+2\alpha)} + Bt^{-(2+\alpha)} \sim t^{-(2+\alpha)} \quad [S5]$$

where  $A$  and  $B$  are constants. As shown in equation S5, the scaling of  $f(t)$  does not change even after the modification of the pair interaction time distribution.

Although we observe only two energy barriers, hence a hyperexponential pair interaction time distribution, the theory in principle could allow the pair interaction time distribution to be an arbitrary sum of exponential distributions  $\sum_i g_i \omega_i e^{-\omega_i t}$ . The same calculation as above gives  $f(t) \sim t^{-(2+\alpha)}$  in this case as well.

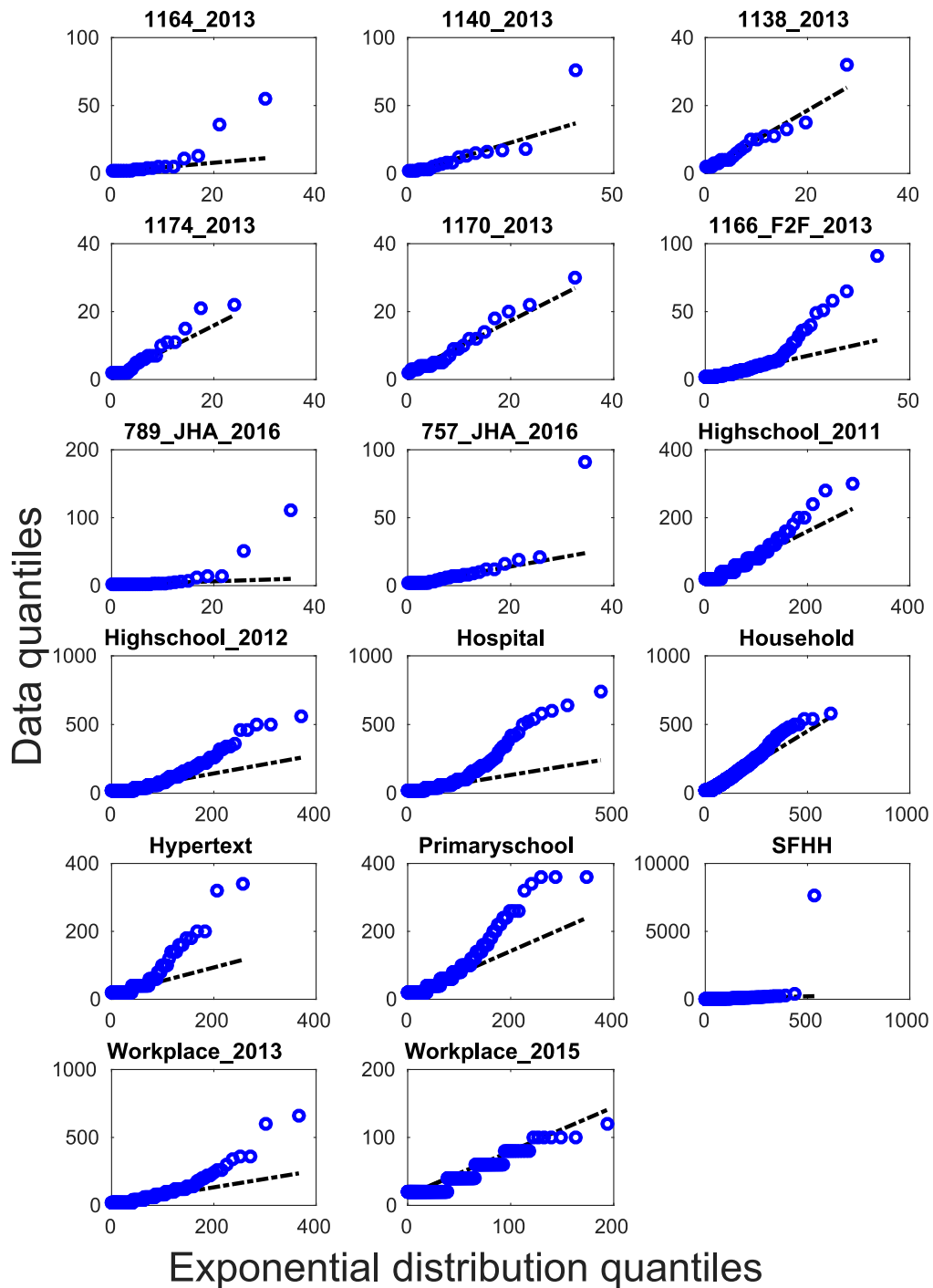


**Fig. S1.** Quantile-quantile plots of the most frequently-interacting pair from each honeybee and human dataset. If the data followed the proposed distribution, the data points would lie on the dashed reference line.

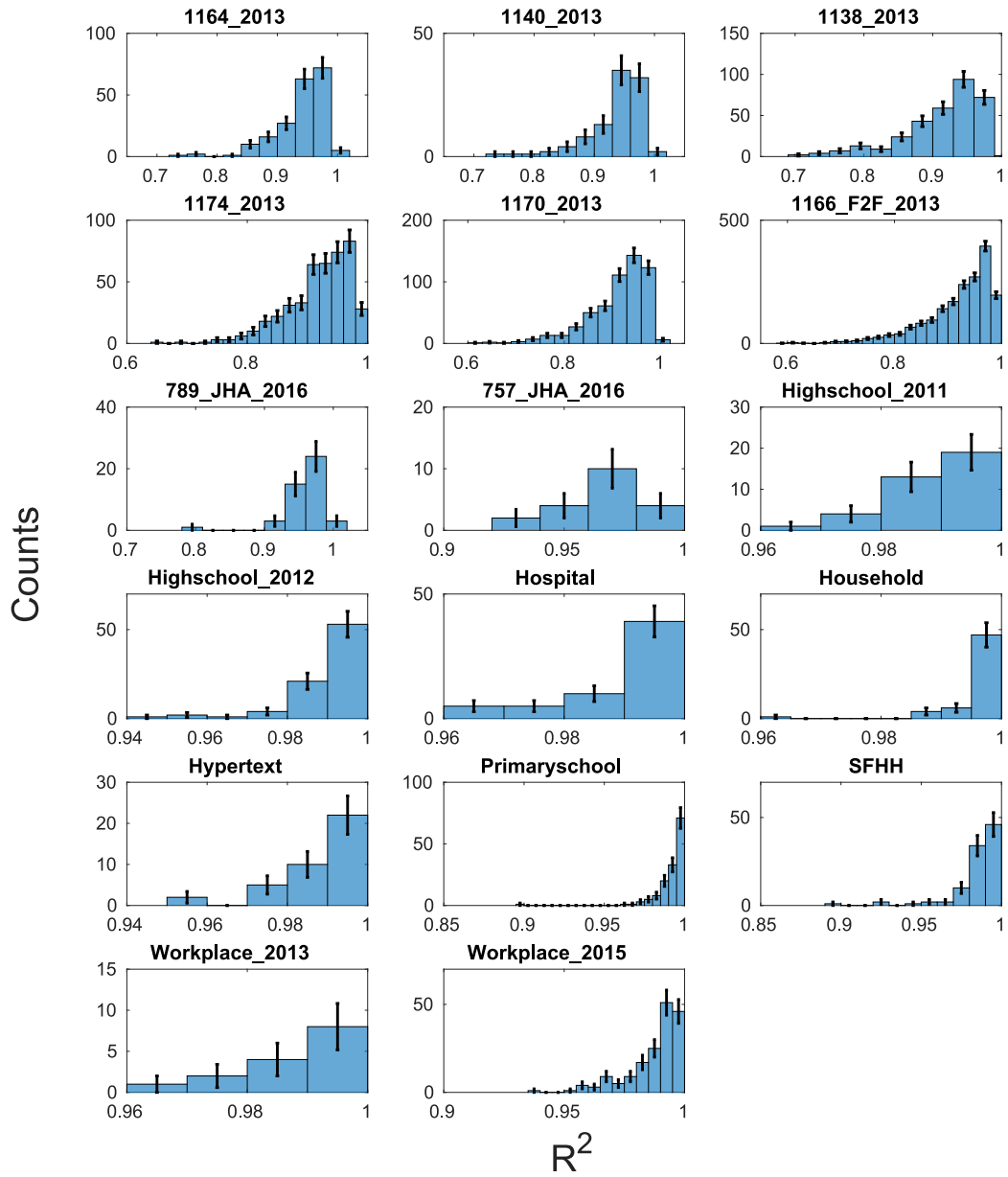


**Fig. S2.** Histogram of  $R^2$  of fitting of the pair interaction time distribution to hyperexponential distribution for all honeybee and human datasets. For all figures, error bars indicate the standard error.

### 55 3. Fitting of the pair interaction time distribution to the hyperexponential distribution.

56 We have fitted the empirical cumulative distribution function (ECDF) of the pair interaction times to the cumulative distribution  
57 function (CDF) of a hyperexponential distribution  $F_{pair}(t) = 1 - ge^{-\omega_1 t} - (1 - g)e^{-\omega_2 t}$ . Fig. S2 shows the histogram of  $R^2$   
58 values of the fitting. It is not a single value but a distribution of values because fitting has been done to each pair and  $R^2$   
59 has been collected from each pair.

60 As shown in Fig. S2, most values of  $R^2$  are close to 1, which means that the pair interaction time distributions are well  
61 represented by a hyperexponential distribution.

62 Fig. S3 shows the histogram of weight  $g$  on the first exponential term in the hyperexponential distribution. Again it shows  
63 not a single value but a distribution of values because the fitting has been done for each pair.

64 The peak near 1 in Fig. S3a-f shows that one of the two exponential terms has a much higher weight than the other in  
65 these datasets. On the other hand, other datasets show more uniform distributions, signifying that both exponential terms,  
66 or both energy barriers, have non-negligible effect on many pairs. The broad distributions in Fig. S3i-q suggest that the  
67 multi-dimensionality of the potential landscape of social interaction is more prominent in humans than in honeybees. Yet, as  
68 shown in Fig. S3g and h, honeybee colonies with partial JHA treatment exhibit similar distributions of weights as humans.  
69 Despite the robust heavy tail in the interaction time distribution, Fig. S3 shows that the presence of honeybees with JHA  
70 treatment does influence the social interaction of honeybees. The precise way that it affects the honeybee social interactions  
71 needs further study and is beyond the scope of this work.

### 72 4. Exponential barrier height distribution.

73 Our model predicts that the barrier height distribution is the extreme value distribution for maxima. However, since the  
74 heavy tail at large time is dominated by high energy barriers, we take the large barrier height limit and obtain the exponential  
75 distribution  $p(E) \sim e^{-(\alpha+1)E}$  where  $E$  is the energy barrier height in units of an effective energy scale that depends on details  
76 of social interactions that are outside the level of description of the present theory and  $\alpha$  is some parameter. Using Kramers'  
77 rate formula  $\omega = \omega_0 e^{-E}$  where  $\omega_0$  is some constant, we express the mean pair interaction time distribution as  $p(\tau) \sim \tau^{-(2+\alpha)}$ .  
78 It has the same scaling as the interaction time distribution  $f(t) \sim t^{-(2+\alpha)}$ . So by comparing the exponent of  $f(t)$  and  $p(\tau)$ , we  
79 verify the exponential energy barrier height distribution.

80 Fig. S4 shows the scaling of the probability densities of interaction time  $f(t)$ , mean pair interaction time from fitting  $p(\tau_{ij})$   
81 and mean pair interaction time from averaging  $p(\tau_i)$  for all honeybee and human datasets. Here the index  $i$  labels a pair,  
82 and the index  $j$  labels an energy barrier.  $\tau_{ij}$  is the mean escape time for each energy barrier and is obtained from fitting of  
83 the pair interaction time distribution. With this index notation, CDF of a hyperexponential distribution to which we have  
84 fitted ECDF of the pair interaction time distribution is written as  $F_i(t) = 1 - g_{i1}e^{-\omega_{i1}t} - g_{i2}e^{-\omega_{i2}t}$  where  $g_{ij}$  is the weight  
85 with  $g_{i2} = 1 - g_{i1}$  and  $\omega_{ij}$  is the rate of each exponential term. These  $g_{i1}$ ,  $\omega_{i1}$  and  $\omega_{i2}$  are fitting parameters. We obtain two  
86 mean pair interaction times  $\tau_{i1}$  and  $\tau_{i2}$  for each pair  $i$  by taking the reciprocal of  $\omega_{i1}$  and  $\omega_{i2}$  respectively. On the other hand,  
87  $\tau_i$  is average of all interaction times for a pair. So  $\tau_i = \frac{1}{n_{i1} + n_{i2}} (\sum_{k=1}^{n_{i1}} t_{i1k} + \sum_{k=1}^{n_{i2}} t_{i2k})$  where  $t_{ijk}$  is the interaction time,  
88 the index  $k$  labels each interaction event, and  $n_{ij}$  is the number of interactions associated with each energy barrier  $j$ . In this  
89 notation, the mean pair interaction time from fitting is  $\tau_{ij} = \frac{1}{n_{ij}} \sum_{k=1}^{n_{ij}} t_{ijk}$ . So the relation between  $\tau_{ij}$  and  $\tau_i$  is written as  
90  $\tau_i = \sum_j g_{ij} \tau_{ij}$  where the weight is  $g_{ij} \equiv n_{ij} / \sum_j n_{ij}$ .

91 In Fig. S4, data points that extend to very large values (such as of order of  $10^{14}$  seconds) were omitted because they are  
92 an artifact from fitting. These outliers correspond to one or two pairs out of all analyzed pairs in the colony. The artifact  
93 arises because the pair interaction time distribution for some pairs is better described by an exponential distribution than a  
94 hyperexponential distribution. In such a case,  $\omega_{i2}$  takes a very small value close to 0 because  $1 - g_{i1}e^{-\omega_{i1}t} - (1 - g_{i1})e^{-\omega_{i2}t} \rightarrow$   
95  $g_{i1}(1 - e^{-\omega_{i1}t})$  for  $\omega_{i2} \rightarrow 0$ . Then taking the value of  $g_{i1}$  close to 1 gives us  $1 - e^{-\omega_{i1}t}$  which is CDF of an exponential  
96 distribution.  $\omega_{i2} \rightarrow 0$  corresponds to  $\tau_{i2} \rightarrow \infty$ , which explains the large  $\tau_{ij}$ 's in some datasets. The pair interaction time  
97 distributions that yield such large  $\tau_{ij}$  indeed have  $g_{ij}$  values close to 1 and are fitted well to exponential distributions.

98 For all datasets,  $p(\tau_{ij})$  exhibits the same scaling as  $f(t)$ , verifying the exponential distribution of energy barriers. On the  
99 other hand, as shown in Fig. S4l and n,  $p(\tau_i)$  doesn't show the same scaling for some datasets, and this feature is discussed in  
100 the next section.

### 101 5. The mean pair interaction time distribution and the stable law.

102 In this section, we discuss the difference between the two kinds of mean pair interaction time distributions  $p(\tau_{ij})$  and  $p(\tau_i)$   
103 to emphasize that  $p(\tau_{ij})$  is the right distribution to use.  $\tau_{ij}$  represents the mean time needed to jump over an energy barrier  
104  $j$ , while  $\tau_i$  is the average of the whole pair interaction times. So the quantity associated with the energy barrier  $E$  through  
105  $\omega = \omega_0 e^{-E}$  is  $\tau_{ij}$ . It would be more accurate to write the Kramers rate formula as  $\omega_{ij} = \omega_0 e^{-E_{ij}}$  according to this notation.  $\tau_i$   
106 is the normalized linear sum of  $\tau_{ij}$ 's.

107 It is very tempting to use  $\tau_i$  instead of  $\tau_{ij}$  because simply averaging the pair interaction times is much easier than fitting  
108 the pair interaction time distributions. Fig. S4 shows whether it matters which mean pair interaction time we use; while  $p(\tau_i)$   
109 has the same scaling as  $p(\tau_{ij})$  and thus as the population interaction time distribution  $f(t)$  for most datasets, it is not the case  
110 for Household (Fig. S4l) and Primaryschool (Fig. S4n). The deviation of  $p(\tau_i)$  is clearer in Primaryschool (Fig. S4n) because  
111 of better statistics associated with the larger dataset. These two particular datasets differ from the rest by having  $f(t)$  that

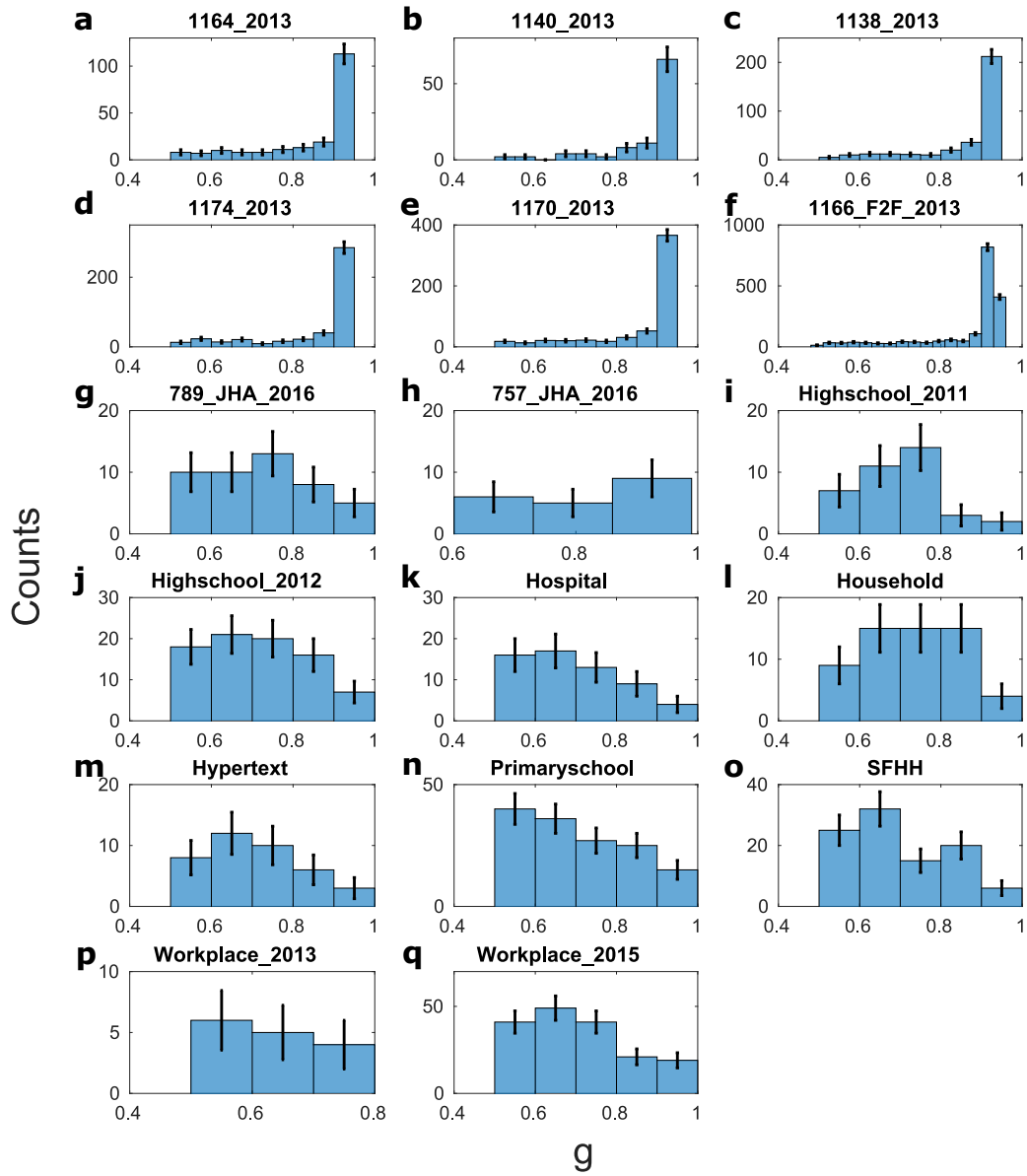


**Fig. S3.** Histogram of weight  $g$  in hyperexponential fitting of the pair interaction time distribution for all honeybee and human datasets.  $g$  can only be between 0.5 and 1. For all figures, error bars indicate the standard error.

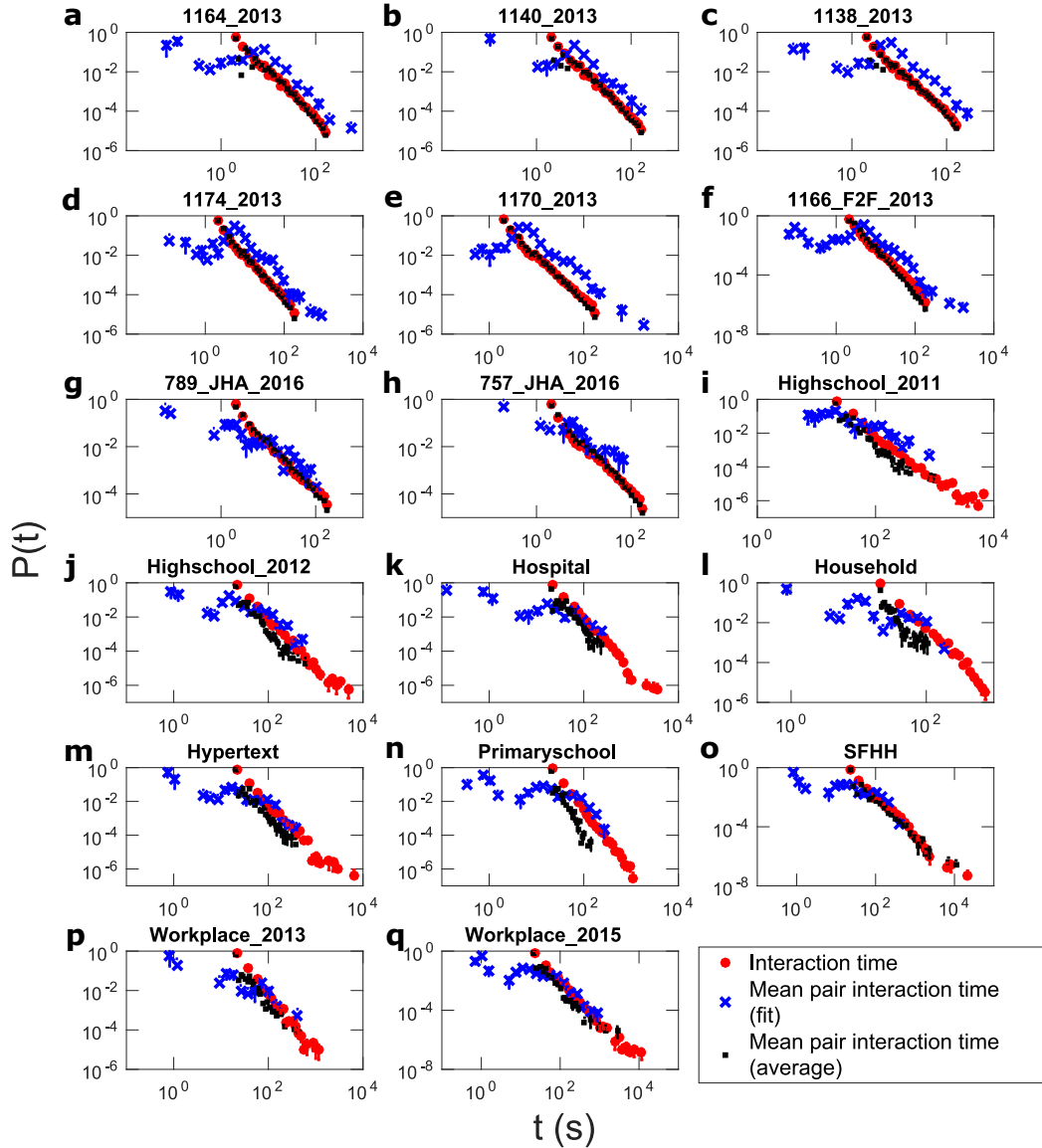


**Fig. S4.** Comparison of scaling between the interaction time distribution and the mean pair interaction time distributions for all honeybee and human datasets. The probability densities of mean pair interaction times obtained by different methods are separately plotted. From **a** to **q**, the number of mean pair interaction times from averaging used to generate the plot is 200723, 143571, 129653, 174317, 212685, 472914, 88441, 76810, 1710, 2220, 1139, 891, 2196, 8316, 9889, 754, 4273, which is the same as the number of detected pairs. The number of mean pair interaction times from fitting used is 197, 99, 328, 443, 561, 1806, 46, 20, 37, 82, 59, 58, 39, 143, 98, 15, 171, which is the same as the number of pairs used for fitting. For all figures, error bars indicate the standard error. Some error bars are not visible because they are smaller than the marker size. Lower error bars for bins of count 1 could not be drawn on a logarithmic scale.

112 decays faster than  $t^{-3}$ ; the exponent of  $f(t)$  of Household is -3.4 and that of Primaryschool is -3.6. The other datasets have  
113  $f(t)$  with exponents from -2 to -3, with specific values are provided in the main text.

114 Now we explain why the value of the exponent of  $f(t)$  is relevant to whether or not  $p(\tau_i)$  has the same scaling as  $p(\tau_{ij})$   
115 by using the so-called stable law (S1), sometimes referred to as the generalized central limit theorem. A probability density  
116 is said to be stable if a linear combination of independent and identically distributed (i.i.d.) random variables drawn from  
117 this probability density is also a random variable from the same probability density up to location and scale parameters. The  
118 normal distribution is a well-known example of a stable distribution. The stable law states that the probability density of  
119 normalized sums of i.i.d. random variables converges to a stable distribution (S1), and specifies the conditions that determine  
120 the appropriate stable distribution. In our case, the random variables are simply the pair interaction times.

121 We are interested in a set of random variables, drawn from an empirical probability distribution that we will call the parent  
122 or source distribution. We wish to know what will be the probability distribution for a linear combination of these variables. If  
123 the parent distribution is stable, then the stable law will imply that the linear combination is also distributed according to the  
124 same distribution. If not then it will be distributed according to a different distribution.

125 The distribution of the linear combination of random variables depends on the asymptotic behavior of the parent distribution.  
126 If the parent distribution  $f(x)$  has the asymptotic behavior  $f(x) \sim x^{-(\alpha+1)}$  with  $\alpha \geq 2$  for large  $x$ , the distribution of the  
127 sums converges to a normal distribution. This result is the central limit theorem. On the other hand, if  $0 < \alpha < 2$ , the parent  
128 distribution itself is stable, so the limit distribution of the sums converges to the parent distribution  $x^{-(\alpha+1)}$ .

129 In our case, the parent distribution is  $p(\tau_{ij})$ , and the distribution of the normalized sums is  $p(\tau_i)$ . The datasets with the  
130 same scaling of  $p(\tau_{ij})$ ,  $p(\tau_i)$  and  $f(t)$  all have  $f(t)$  with exponents from -2 to -3. According to the theory in the main text,  $f(t)$   
131 and  $p(\tau_{ij})$  always have the same exponents, which is verified by all the datasets in Fig. S4; thus  $p(\tau_{ij})$  has exponents in the  
132 range from -2 to -3. It can be re-written as  $p(\tau_{ij}) \sim \tau_{ij}^{-(\alpha+1)}$  with  $1 < \alpha < 2$ . Indeed, we see that  $\alpha$  is in the range where  
133  $p(\tau_{ij})$  is stable, and so we expect the same scaling between  $p(\tau_i)$  and  $p(\tau_{ij})$ , assuming that the variables are indeed i.i.d. In  
134 conclusion,  $f(t)$  has the same scaling as  $p(\tau_{ij})$  due to our theory, while  $p(\tau_{ij})$  and  $p(\tau_i)$  have the same scaling because  $p(\tau_{ij})$  is  
135 the parent distribution of  $p(\tau_i)$ . Thus all three variables have the same scaling when  $\alpha + 1$  is in the range from -2 to -3.

136 On the other hand, Household (Fig. S4) and Primaryschool (Fig. S4n) have  $f(t)$ , and thus  $p(\tau_{ij})$ , with exponents -3.4  
137 and -3.6 respectively. These exponents correspond to  $\alpha + 1$ . For these datasets,  $\alpha > 2$ , showing that  $p(\tau_{ij})$  is not a stable  
138 distribution. Therefore, the stable law predicts that  $p(\tau_i)$  does not have the same scaling as  $p(\tau_{ij})$  and  $f(t)$ . The deviation of  
139  $p(\tau_i)$  from the other two distributions in Fig. S4l and n is consistent with this prediction.

140 Although the stable law predicts that the probability density of the normalized sum of i.i.d. random variables that are  
141 not stable converges to a Gaussian,  $p(\tau_i)$  is not Gaussian as shown in Fig. S4l and n. It is not Gaussian because the number  
142 of summed  $\tau_{ij}$  is only two, as there are two energy barriers for each pair. The convergence to a Gaussian only occurs if the  
143 number of summands is large (e.g. more than 10). In addition, even if the number of summands were large, burstiness of  
144 temporal social networks of honeybees and humans suggests that  $\tau_{ij}$  could be not i.i.d. Then  $p(\tau_i)$  would be expected to exhibit  
145 an exponential tail rather than a Gaussian tail, because the distribution of the normalized sum of correlated random variables  
146 converges to the Fisher-Tippett-Gumbel distribution, which has an exponential tail (S2).

147 In summary,  $f(t)$  and  $p(\tau_{ij})$  always have the same scaling, as predicted by our theory. However, as demonstrated in Fig.  
148 S4l and n,  $p(\tau_i)$  may or may not have the same scaling as  $f(t)$  depending on the exponent that characterizes the asymptotic  
149 behavior of  $f(t)$ , in accord with the stable law. This observation shows that we cannot ignore the fact that there are two energy  
150 barriers per pair, and we indeed need to obtain the mean pair interaction times by fitting the pair interaction time distribution to  
151 the hyperexponential function.

152 Note that the stable law does not hold between  $f(t)$  and  $p(\tau_{ij})$  although they have the same exponent.  $\tau_{ij}$  is a normalized  
153 sum of pair interaction times associated with one energy barrier whose probability density is exponential. So the parent  
154 distribution for  $\tau_{ij}$  is not  $f(t)$ . Furthermore, each  $\tau_{ij}$  has its own parent distribution labeled by indices  $i$  and  $j$ , which is an  
155 exponential distribution with different parameter values. The stable law concerns the normalized sum of random variables from  
156 the same probability density. Therefore, one cannot predict the form of  $p(\tau_{ij})$  from  $f(t)$ .

157 Conversely, our theory is only able to predict the form of  $f(t)$  from  $p(\tau_{ij})$  precisely because  $f(t)$  is not the parent distribution  
158 for  $\tau_{ij}$  and so the stable law does not hold between them. As a result, the scaling of  $p(\tau_{ij})$  is purely determined by  $p(E_{ij})$ .

## 159 6. Lorenz plots.

160 Heterogeneity or variability in the population is represented by the barrier height distribution in our model. However, the  
161 model does not dictate whether the barrier height is determined by a specific pair or a particular individual, which poses the  
162 question about the individuality in social interaction. To explore the effect of individuality in a way that is independent of our  
163 theory, we have calculated the Gini coefficients (S3) for the total number of interactions and the total number of partners in  
164 addition to the total interaction time shown in the main text. We have chosen the Gini coefficient to quantify the different  
165 degree of dominance in social interactions by each individual because we are analyzing interaction times, which are shared  
166 between a pair, and thus it is nontrivial to decouple individual contribution.

167 Fig. S5 shows the Lorenz plots (S4) for the total number of interactions and the total number of partners of honeybees  
168 and humans. The larger deviation from the reference line in Fig. S5b and d than in Fig. S5a and c respectively indicates that  
169 individual differences are larger in human communities than honeybee communities. However, Fig. S5a and c still show a  
170 deviation from the straight line, signifying that honeybee individuals are different. This result still does not tell us how much  
171 individuality contributes to social interaction. Given that the energy barrier is a pairwise property, we can only tell that the



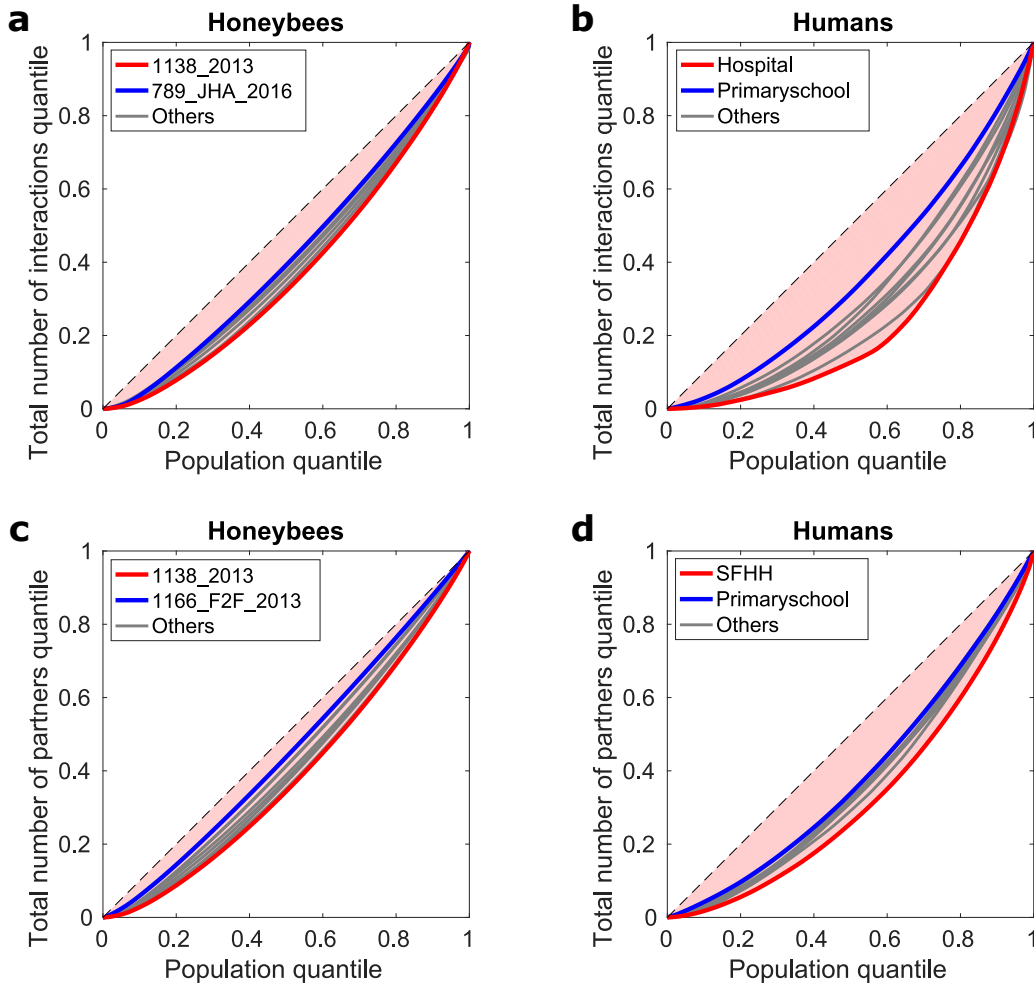


**Fig. S5.** Lorenz plots for total number of interactions and total number of partners for honeybees and humans. **a.** Gini coefficients for total number of interactions of honeybees are following. 1164\_2013: 0.2125, 1140\_2013: 0.1823, 1138\_2013: 0.2526, 1174\_2013: 0.2462, 1170\_2013: 0.2362, 1166\_F2F\_2013: 0.1949, 789\_JHA\_2016: 0.1609, 757\_JHA\_2016: 0.1667. **b.** Gini coefficients for total number of interactions of humans are following. Highschool\_2011: 0.3509, Highschool\_2012: 0.4361, Hospital: 0.5293, Household: 0.4992, Hypertext: 0.4089, Primaryschool: 0.2595, SFHH: 0.4410, Workplace\_2013: 0.4011, Workplace\_2015: 0.3426. **c.** Gini coefficients for total number of partners of honeybees are following. 1164\_2013: 0.1758, 1140\_2013: 0.1619, 1138\_2013: 0.2222, 1174\_2013: 0.2081, 1170\_2013: 0.1897, 1166\_F2F\_2016: 0.0916, 789\_JHA\_2016: 0.1284, 757\_JHA\_2016: 0.1301. **d.** Gini coefficients for total number of partners of humans are following. Highschool\_2011: 0.2612, Highschool\_2012: 0.2538, Hospital: 0.2828, Household: 0.2498, Hypertext: 0.2643, Primaryschool: 0.2215, SFHH: 0.3474, Workplace\_2013: 0.2537, Workplace\_2015: 0.2243.

172 pairwise heterogeneity is essential for the heavy tail to appear in the interaction time distribution, as demonstrated in this  
173 report, but whether the pairwise heterogeneity is purely a property of a pair independent of individuals forming the pair is still  
174 open for further study.

## 175 **References**

- 176 [S1] Gnedenko BV, Kolmogorov AN (1954) *Limit Distributions for Sums of Independent Random Variables*. (Addison-Wesley).  
177 [S2] Bertin E, Clusel M (2006) Generalized extreme value statistics and sum of correlated variables. *J. Phys. A: Math. Gen.*  
178 39(24):7607–7619.  
179 [S3] Gini C (1912) Variabilità e mutabilità (variability and mutability). *Reprinted in Memorie di metodologica statistica (Ed.*  
180 *Pizetti E, Salvemini, T). Rome: Libreria Eredi Virgilio Veschi (1955) ed. Bologna.*  
181 [S4] Lorenz MO (1905) Methods of measuring the concentration of wealth. *Publications of the American statistical association*  
182 9(70):209–219.